Folded Waveguide: a New Kind of Radio-Frequency Antenna

YE Wei-wei(叶薇薇), LI Jian-gang(李建刚), CUI Ning-zhou (崔凝卓), ZHAO Yan-ping(赵燕平)
Institute of Plasma Physics, Chinese Academy of Sciences, Hefei 230031

(Received 4 October 1998)

The properties of folded waveguide (FWG) couplers are researched. Firstly, the electromagnetic fields inside and outside of the FWG are analyzed theoretically. After substituting the relevant data, numerical results and corresponding two-dimensional and three-dimensional wave field figures are achieved. Secondly, in our scale model, series of experiments are carried out. The coupling and matching between the antenna and the coaxial line are examined. The experimental results demonstrate that FWG antenna can be used in ion cyclotron range of frequencies heating in tokamak with high power coupling efficiency.

PACS: 52.50.Gj, 52.40.Fd, 52.55.Fa

Plasma heating in ion cyclotron range of frequencies (ICRF) has been applied with a high degree of success to a number of experimental fusion devices.[1] Until now, inductive loops have usually been used to launch power for plasma heating in ICRF. Loop antenna has been successful in coupling average power flux of $0.3-1\,\mathrm{kW/cm^2}$ while the future fusion reactors need at least $2\,\mathrm{kW/cm^2}$. The result of low hybrid heating experiments shows that the coupling average power fluxes of rectangular waveguide antenna can reach $5-10\,\mathrm{kW/cm^2}$ when the waveguide is coupling powers up to 1 MW.[2] Thus, the waveguide antennas can be used in coupling high power into plasma. Since the ion cyclotron range of frequencies are low, the consequent simple rectangular waveguide is too large to be installed in tokamak. Owens[1] suggested the concept of folded waveguide antenna in ICRF heating.

The basic idea involves folding a simple rectangular waveguide that has a much longer width than height to form a more compact structure as Fig. 1. shows. When the path length of the folded waveguide (FWG), which is the center line around the folders, equals half a free-space wavelength, it is cut-off. So for the FWG that has the same outside size, the more folds of it, the lower cut-off frequency.

To make it serve as a wave launcher in ICRF heating, two important parts which are suggested by Owens are added to the FWG.[1] The polarizing plate attached at the front mouth of FWG and the adjustable shorting back plate on the back mouth of the waveguide as shown in Fig. 1.

Polarizing plate is a thin metal that has serial rectangular apertures. Different position of the apertures in the plate forms different types of polarizing plate. In our scaling experiments, standard polarizing plate is used. It has apertures in every other fold, which make the complicated fields in the FWG unidirectional. Because the fields in adjacent folds have counter directions, the aperture allows only fields of same direction to pass while fields of opposite direction are reflected. This process can make a favorable wavenumber spectrum.

Shorting back plate is placed on the back end of the FWG to make it convert to a folded rectangular cavity. The fields in the cavity launch though the front mouth. Therefore, the folded waveguide can be used in ICRF heating. The distance from the back plate to

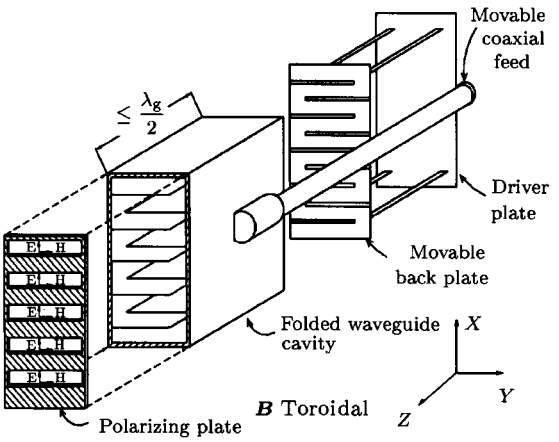

Fig. 1. Folded waveguide coupler consists of FWG, polarizing plate and shorting back plate.

the front mouth of FWG is about one-half of waveguide wavelength so the electric fields of wave are small while the parallel magnetic fields there are near maximum. This wave field pattern makes a good match with the plasma surface fields for the low impedance of the plasma surface.

The resonant condition for such a rectangular cavity is

$$\left(\frac{2f}{c}\right)^2 = \left(\frac{1}{L}\right)^2 + \left(\frac{1}{W}\right)^2, \tag{1}$$

where c is the velocity of light, f the resonant frequency, L the length of the cavity from front to back, W the effective width of the cavity.

For calculating the wave fields of the FWG coupler, we divided the whole region into two parts: the region inside the FWG and the region outside the FWG that cover the vacuum area between the front mouth of FWG to the plasma surface. Equivalent unfolded waveguide model is used to calculate the wave fields in the former region and the following equations are got:[1]

$$E_x = \sum_{m=2}^{\infty} A_{0m} \mathrm{e}^{\alpha_{0m} z'} \frac{\mathrm{e}^{-2\alpha_{0m}(z'+d)} - 1}{\mathrm{e}^{-2\alpha_{0m} d} - 1} \sin\left(\frac{m\pi y'}{b}\right) + A_{01} \frac{\sin[\beta_{01}(z'+d)]}{\sin(\beta_{01} d)} \sin\left(\frac{\pi y'}{b}\right), \tag{2}$$

©by the Chinese Physical Society

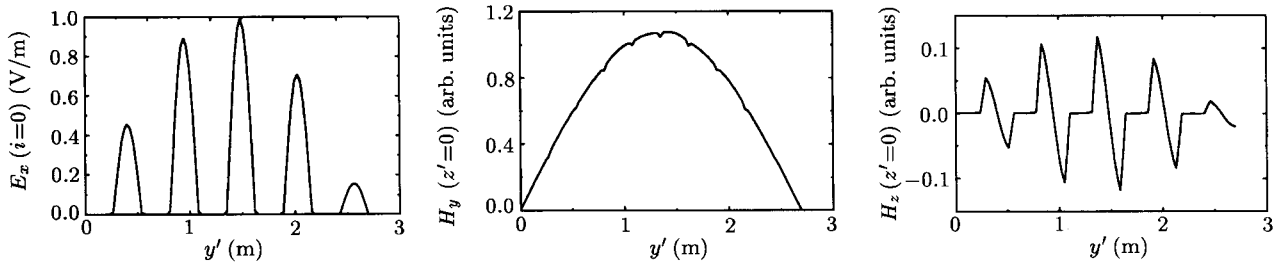

Fig. 2. Wave fields at the mouth of the FWG. (a) Vertical electric field, (d) parallel magnetic field, (c) radial magnetic field. The equivalent unfolded waveguide model has been used in the calculation. Parameters are: $b = 2.7$ m, $a = 0.032$ m, $N = 5$, $v = 0.1$ m, $f = 125.7$ MHz, $E_0 = 1$ V/m.

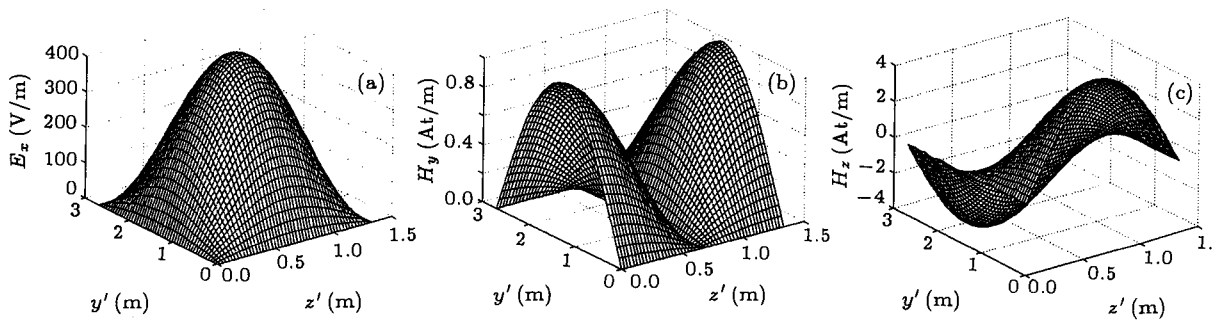

Fig. 3. Three-dimensional plots of wave fields within the volume of the FWG. (a) Vertical electric field, (b) parallel magnetic field, (c) radial magnetic field. The parameters are the same as those of Fig. 2.

$$H_y = \sum_{m=2}^{\infty} A_{0m} \mathrm{e}^{\alpha_{0m} z'} \left(\frac{j\alpha_{0m}}{\omega\mu}\right) \frac{\mathrm{e}^{-2\alpha_{0m}(z'+d)} + 1}{\mathrm{e}^{-2\alpha_{0m} d} - 1} \cdot \sin\left(\frac{m\pi y'}{b}\right) + A_{01} \frac{j\beta_{01}}{\omega\mu} \frac{\cos[\beta_{01}(z'+d)]}{\sin(\beta_{01} d)} \sin\left(\frac{\pi y'}{b}\right), \tag{3}$$

$$H_z = \sum_{m=2}^{\infty} A_{0m} \mathrm{e}^{\alpha_{0m} z'} \left(\frac{jm\pi}{bk_0}\right) \frac{\mathrm{e}^{-2\alpha_{0m}(z'+d)} - 1}{\mathrm{e}^{-2\alpha_{0m} d} - 1} \cdot \cos\left(\frac{m\pi y'}{b}\right) + A_{01} \frac{j\pi}{ak_0} \frac{\sin[\beta_{01}(z'+d)]}{\sin(\beta_{01} d)} \cos\left(\frac{\pi y'}{b}\right), \tag{4}$$

where x correspond to the poloidal direction, y the toroidal direction, z the radial direction, a is the height of one fold, b is the effective width of the equivalent unfolded waveguide cross-section, d is the length from the front of waveguide to the back end of it.

$$\eta = \left(\frac{\mu}{\varepsilon}\right)^{1/2}, \quad k_c = \left[\left(\frac{n\pi}{a}\right)^2 + \left(\frac{m\pi}{b}\right)^2\right]^{1/2},$$

$$\beta_{nm} = (k_0^2 - k_c^2)^{1/2}, \quad j\alpha_{0m} = \beta_{0m},$$

where β_{nm} is the transmission coefficient of the TE_{nm} mode. To calculate the fields in the latter region, aperture-excited cavity model is applied:[1]

$$E_x = \sum_{n=0}^{\infty} \sum_{m=1}^{\infty} \gamma_{nm} \frac{\mathrm{e}^{-\sigma_{nm}(z-2v)} - \mathrm{e}^{\sigma_{nm} z}}{\mathrm{e}^{2\sigma_{nm} v} - 1} \cdot \cos\left(\frac{n\pi x}{u}\right) \sin\left(\frac{m\pi y}{w}\right), \tag{5}$$

$$H_y = \sum_{n=0}^{\infty} \sum_{m=1}^{\infty} -\gamma_{nm} \left(\frac{j\sigma_{nm}}{\omega\mu}\right) \frac{\mathrm{e}^{-\sigma_{nm}(z-2v)} + \mathrm{e}^{\sigma_{nm} z}}{\mathrm{e}^{2\sigma_{nm} v} - 1} \cdot \cos\left(\frac{n\pi x}{u}\right) \sin\left(\frac{m\pi y}{w}\right), \tag{6}$$

$$H_z = \sum_{n=0}^{\infty} \sum_{m=1}^{\infty} \gamma_{nm} \left(\frac{w}{m\pi}\right) \left(\frac{k_0^2 + \sigma_{nm}^2}{j\omega\mu}\right) \cdot \frac{\mathrm{e}^{-\sigma_{nm}(z-2v)} + \mathrm{e}^{\sigma_{nm} z}}{\mathrm{e}^{2\sigma_{nm} v} - 1} \cos\left(\frac{n\pi x}{u}\right) \cos\left(\frac{m\pi y}{w}\right), \tag{7}$$

where u and w are the height and width of the aperture-excited cavity, γ_{nm} is the Fourier coefficient in our calculation.

$$j\sigma_{nm} = k_{nm}, \quad k_{nm} = \left[k_0^2 - \left(\frac{n\pi}{u}\right)^2 - \left(\frac{m\pi}{w}\right)^2\right]^{1/2}.$$

A scaling model of ten folds was built to research the properties of the FWG.[3] Its outside length is 1.33 m, the effective width is 2.7 m, and its outside height is 0.33 m. Here the shorting back plate is fixed. This scheme not only simplifies the coupler mechanics but also improves its current handling at the shorting back plate. Through Eq. (1), the resonance of FWG can be achieved by tuning the applied frequency. For our scaling model, the resonant frequency is 125.7 MHz.

The numerical results of our scaling model of the eigenmode fields that are given by Eqs. (2)–(7) are shown in Figs. 2–4. Figure 2 shows the wave fields at

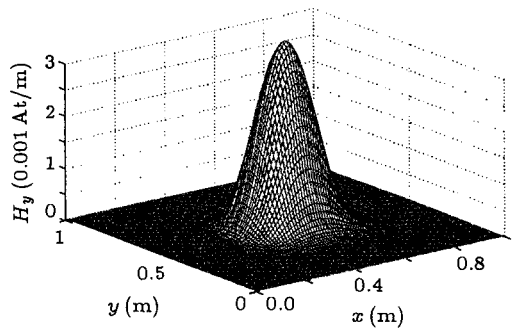

Fig. 4. H_y field at the surface of the plasma $z = v$ for the FWG. Parameters are $u = w = 1.0\,\mathrm{m}$, $v = 0.1\,\mathrm{m}$.

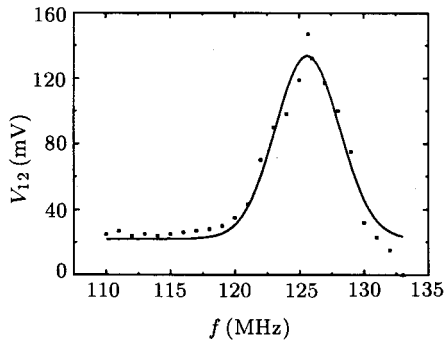

Fig. 5. Relation of resonance of FWG and frequency of the signal generator.

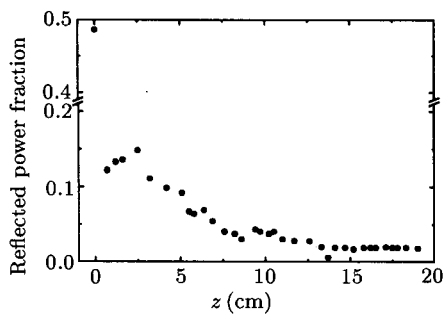

Fig. 6. Match as the vane toucher varied around the optimum position, where z is the position of vane toucher from the back plate.

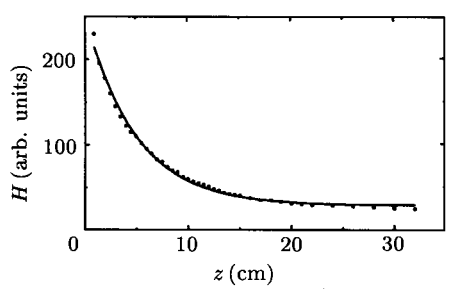

Fig. 7. Radial variation of the RF magnetic field in front of FWG, where z is the position of vane toucher from the back plate.

the mouth of the coupler for the equivalent unfolded waveguide fields given by Eqs. (2)–(4). In this case E_0 has been taken to be 1.0 V/m. The H fields are given in units of At/m, and the E field is given in V/m in the figure. The fields in Fig. 2 show apparent differences from those of the simple rectangular waveguide. In a given aperture, the H_z field is positive on one side and negative on the other side while H_y is always positive. The total magnetic field therefore fringes into the plasma region. It is the fringe field that couples power to the plasma.

The wave fields throughout the volume of the folded waveguide are shown in the three-dimensional plots of Fig. 3. The equivalent unfolded waveguide model is also used to calculate the wave fields shown in these plots. The fine structure of the fields at the coupler mouth caused by the aperture is seen to disappear about 10 cm axially down the waveguide. This is because the fine structure is a result of the excitation of high mode waves, which are evanescent. The field distribution becomes that of TE_{10} rectangular cavity mode for axial distances greater than 10 cm from the coupler mouth.

Figure 4 is a plot of the toroidal H field at the surface of the plasma that is taken to be 10 cm in front of the mouth of the coupler in our calculation. The field has been calculated by using the aperture-coupled cavity model. It is observed in the figure that the toroidal magnetic field goes to zero well inside if the walls that surround it along the $x - y$ parameter. This shows the solutions are relatively insensitive to the position of these enclosing sidewalls as long as they are separated from the coupler mouth by approximately the distance from the coupler mouth to the plasma.

Except for the theoretical and numerical analysis, serials of experiments are also done on the scaling model.[4]

We changed the frequency of signal generator, and the corresponding voltage difference between the incident wave and reflected wave is gotten, as shown in Fig. 5. It can be seen that the resonance of the FWG happens while the frequency of signal is 125.7 MHz, which fits with our numerical result fairly well. Through the plot, the quality factor is calculated $Q = 36$.

Radio-frequency power is brought into the FWG via a coaxial line that makes contact with the central vane by means of a vane toucher. Vane toucher can be moved along the vane to match the FWG to the characteristic impedance of the coaxial line. The optimum position for the vane toucher, which led to the lowest reflected power, can be determined by observing the match as the position is changed. Figure 6 shows the optimum position is where the length from the vane toucher to the back plate is 13.7 cm. In that position, the minimum of the reflected power is −21.9 db.

The magnetic fields in front of the FWG are measured using small loop probe. The radial variation of the fields in shown in Fig. 7. This figure shows that the field of the FWG is very much like that of a loop antenna. The data can be fitted by an exponential function.

REFERENCES

[1] T. L. Owens, IEEE Trans. Plasma Sci. 14 (1986) 934.
[2] J. L. Lee, J. E. Scharer and B. M. Jost, IEEE Trans. Plasma Sci. 16 (1988) 645.
[3] T. S. Bigelow *et al.*, *Proceedings of the IEEE/NPS Symposium on Fusion Engineering* (Hyannis, Massachusettes, Oct. 11–15, 1993).
[4] G. R. Haste *et al.*, Fusion Eng. Des. 24 (1994) 191.